Nanoscale Advances

ROYAL SOCIETY OF CHEMISTRY

PAPER

View Article Online
View Journal | View Issue

Cite this: *Nanoscale Adv.*, 2024, **6**, 5874

Preparation of a minocycline polymer micelle thermosensitive gel and its application in spinal cord injury

Jun Gu,[ab] Xiaohu Cai,[ac] Faisal Raza,[d] Hajra Zafar,[d] Bo Chu,[b] Haitao Yuan,[b] Tianqi Wang,[b] Jiapeng Wang[e] and Xiaojun Feng*[ab]

Neuroprotection is an important approach for the treatment of spinal cord injury (SCI). Minocycline (MC), a known neuroprotective agent, has been utilized for SCI treatment, but its therapeutic effect is limited by instability and low bioavailability. Herein, we developed an innovative micellar thermosensitive hydrogel (MCPP-M-gel) that encapsulates MC in polyethylene glycol (PEG)–poly(lactide-*co*-glycolic acid) (PLGA) micelles to enhance its therapeutic efficacy in a rat model of SCI. The micelles were synthesized *via* the thin-film hydration method and characterized for encapsulation efficiency, particle size, zeta potential, and polydispersity index (PDI). MCPP-M-gel demonstrated favorable physico-mechanical properties and extended MC release over 72 hours *in vitro* without cytotoxic effects on neural crest-derived ectoderm mesenchymal stem cells (EMSCs). Thereafter, MC, MCPP-M, MCPP-M-gel and a blank micellar thermosensitive gel were injected into the injured site of SCI rats. Histopathological evaluation demonstrated that MCPP-M-gel could promote neuronal regeneration at the injured site of the SC after 28 days. Immunofluorescence techniques revealed that MCPP-M-gel increased the expression of neuronal class III β-tubulin (Tuj1), myelin basic protein (MBP), growth-associated protein 43 (GAP43), neurofilament protein-200 (NF-200) and nestin as well as reduced glial-fibrillary acidic protein (GFAP) expression in damaged areas of the SC. In conclusion, this study innovatively developed MCPP-M-gel based on a PEG–PLGA copolymer as a biomaterial, laying a solid foundation for further research and application of MCPP-M-gel in SCI models or other neurodegenerative diseases.

Received 29th July 2024
Accepted 15th September 2024

DOI: 10.1039/d4na00625a

rsc.li/nanoscale-advances

Introduction

The spinal cord (SC) can be injured through mechanical trauma, which induces a cataclysmal condition of neurons. This is commonly known as spinal cord injury (SCI), which can have an enormous socio-economic impact on affected individuals. It is a condition that can trigger a cascade of consequences such as the generation of free radicals, perturbation of ionic balance, vascular alterations, response to inflammation and apoptosis.[1] The aforementioned events are degenerative and normally associated with neuronal loss and axonal devolution, culminating in progressive damage to neuronal tissues and SC functional impairment.[2] In recent years, scientists have explored preclinical models of SCI to investigate numerous drugs that have the potential to repair injured tissue and enhance the recovery of SC functions.[3,4] From a preclinical point of view, the complex nature of SCI has hampered the successful development of therapeutic interventions for this condition. This is because only few of them have been translated into clinical settings, albeit with limited success, probably because only one aspect of SCI has been targeted.[5] Hence, for effective treatment of SCI, prospective drugs should be developed to target multiple aspects of the injury to facilitate neuroprotection, neuronal regeneration and recovery of SC function. Besides, long-term use of conventional medications for SCI treatment can cause various drug-related medical problems for patients. Notable among these medical problems are dyslipidemia, hypertension, anxiety/depression, osteoarthritis and osteopenia/osteoporosis.[6] Novel therapeutic strategies are required for the effective treatment of SCI. At present, neuroprotective medications that block sodium channels (riluzole) and act as antioxidants (vitamin E) and anti-inflammatory agents (curcumin, methylprednisolone and minocycline), among others, have been widely explored to treat SCI.[7]

As a derivative of tetracycline, minocycline (MC) is considered an antibiotic that is available clinically with non-antibiotic beneficial effects such as anti-apoptosis, neuroprotection, anti-oxidation and anti-inflammation.[8] Because of its neuroprotective potential, MC has widely been used to treat disorders

[a]*School of Medicine, Yangzhou University, Yangzhou, Jiangsu 225009, China. E-mail: featherinwind81@163.com*
[b]*Department of Orthopedics, Xishan People's Hospital, Wuxi, Jiangsu 204105, China*
[c]*Department of Rehabilitation, Xishan People's Hospital, Wuxi, Jiangsu 204105, China*
[d]*School of Pharmacy, Shanghai Jiao Tong University, Shanghai 200240, China*
[e]*School of Pharmacy, Jiangsu University, Zhenjiang, Jiangsu 212013, China*

of neurons: Alzheimer's disease, amyotrophic lateral, multiple sclerosis, Parkinson's disease and SCI.[9–11] In particular, MC demonstrated the potential to increase levels of anti-inflammatory cytokines and reduce pro-inflammatory factors in animal models of SCI.[12] In another work, the authors showed that MC decreased the apoptotic rate in oligodendrocytes and neurons by stimulating the production of microglial pro-nerve factor, inhibiting activated caspases and suppressing mitochondrial cytochrome c release.[13,14] Evidently, scientists have discovered that the cascade of secondary apoptosis that occurs after acute SCI plays vital roles in SCI pathogenesis.[15] In this same work, the authors showed that Bcl-2 plays a very important role in the death of nerve cells after SCI.[15] In particular, Bcl-2 is considered an anti-apoptotic protein that can inhibit or effectively prevent the apoptosis caused by various pathways after SCI by promoting the repair of injured nerve tissue and neuroprotection.[16] Indeed, Bcl-2 plays a neuroprotective role in SCI by inhibiting neuronal cell death. Currently, studies have shown that MC intervention could inhibit neuronal apoptosis by increasing Bcl-2 expression, thereby playing a therapeutic role in SCI.[17] More importantly, the highly lipophilic nature of MC may facilitate the drug to readily cross the blood–brain barrier and subsequently distribute into the tissues of the central nervous system and cerebrospinal fluid.[18] Nonetheless, clinical applications of MC are limited by its systemic toxicity[19] and possibly its inability to penetrate the blood–spinal cord barrier, which prevents effective delivery of conventional drugs to the SC, especially when administered systemically, orally or into the peridural space.[20,21] To overcome the above challenges, scientists through preclinical studies have explored the potential of nanomaterials, such as micelles and hydrogels, to effectively target drugs to the injured site of SC. The nanotechnological-based delivery system of drugs has various advantages, such as increased aqueous solubility, decreased toxicity, enhanced biological availability and prolonged circulation time in the bloodstream.[22] Most lipophilic drugs have been encapsulated using poly(lactate-*co*-glycolic acid) (PLGA), a polymer that has been approved by the Food and Drug Administration (FDA) because it offers advantages, such as increased bioavailability of drugs, reduced toxicity of the system and good biodegradability.[23] Nonetheless, PLGA applications are limited because of the easy opsonization and rapid clearance of polymer-based drugs by the reticulo-endothelial system (RES) after intravenous administration. Therefore, formulation scientists usually conjugate hydrophobic PLGA with hydrophilic polyethylene glycol (PEG) to fabricate a co-polymeric (PLGA–PEG) block platform that is amphiphilic. Importantly, PEGylation of PLGA-based nanoparticles resulted in minimal neurotoxicity and enhanced stability of bioactive deoxyribonucleic acid (DNA) in primary neurons of the hippocampus.[24] Besides, PLGA–PEG co-polymer has been employed by other scientists to fabricate thermosensitive nanoplatforms for applications in SCI.[25] In an aqueous milieu, amphipathic polymers can assemble to spontaneously produce nanostructured polymeric micelles, which have the advantages of increased physical stability, prolonged release, targeted delivery, greater bioactivity, solubilization of active compounds or high stability of the incorporated drug.[26] The available literature has posited that polysialic acid-based polymeric micelles loaded with MC could substantially lower the formation of scars and reduce injury to nerve and myelin sheaths through anti-inflammation and anti-oxidation.[27] In another study, polymeric micelles developed with scar tissue targeting ability peptides, such as cysteine–alanine–glutamine–lysine (CAQK), could treat SCI through the specific delivery of apocynin to lesion tissue.[28] Biodegradable amphipathic micelles were developed by Wang and colleagues,[29] which enhanced the synergistic neuroprotective activity of dexamethasone acetate and glucocorticoid in the SCI model. Notwithstanding the potential of these formulations, their shortfalls hamper their clinical applications in SCI. Specifically, the instability of polymeric micelles in the blood causes the rapid release of MC after administration, which affects the accumulation of the drug in the injured site of SC.[30,31] Thus, the search for ideal nanocarriers of MC to target the drug to SC is ongoing.

As a category of polymers, hydrogels absorb water to form a 3-dimensional network through their hydrophilic groups, which have the morphology of flexible tissue with similarity to the extracellular matrix features.[32,33] Common biomaterials, such as hydrogels, significantly affect SCI treatment because they are biocompatible with some of them displaying electrical conductivity that is compatible with tissues of SC.[34] Hydrogels have been employed to incorporate several cells or active compounds and drugs with the potential to treat SCI because of their greater capability to deliver drugs in a prolonged fashion to target sites.[34] Besides, the plasticity and high biocompatibility nature of hydrogels can facilitate the accumulation of the polymers at the defective SC and the continuous release of drugs, such as MC.[34] More importantly, scientists have reported the potential of hydrogels to support the growth of axons and their regeneration.[35] Thus, scientists can leverage the advantages of micelles and hydrogels to design nanocarriers that are more compatible with biological stimuli.

Recently, scientists have renewed their interest in the *in situ* formation of hydrogel, which occurs as a result of the transformation of aqueous polymeric solutions into gels due to alterations in milieu conditions, such as pH and temperature.[36] It has been posited that this type of hydrogel can provide several advantages compared with conventional ones when they are formed under conditions of physiology and maintain their integrity for a desired period. In recent times, researchers have developed a thermosensitive micellar-hydrogel (MH) system that displays the advantages of both polymeric micelles and hydrogels, which has attracted much interest in tissue engineering.[37] Thus, this system was developed to achieve sustained and long-lasting delivery of hydrophobic drugs *via* the formation of a hybrid micelle-cross-linked hydrogel, which potentially serves as a reservoir of lipophilic solutes.[38] Particularly, the self-assembling of hydrophilic–hydrophobic co-polymer into hydrogel occurs in an aqueous environment and under physiological conditions, wherein it can flow like micelles in a concentration-dependent fashion.[39] Various studies have indicated that the MH system has been developed with different materials for various applications. For instance, Qin and colleagues developed an MH system for the sustained delivery of celastrol and its application in renal fibrosis.[38] In another

work, Sun and co-authors fabricated an MH system that demonstrated the increased anti-breast cancer effect of quercetin.[40] In addition, Xu and co-experimenters fabricated a thermosensitive MH system to incorporate and deliver docetaxel to the intra-tumoral site.[41] Additionally, Yi *et al.* developed an MC-loaded hydrogel with F127 as the polymer for application in periodontal diseases.[42] As one of the most broadly utilized thermos-reversible gelling polymers for hydrogel development, the PEG-PGLA block has been found to demonstrate excellent biocompatibility and biodegradability in terms of delivery of drugs.[43]

Based on previous studies, this study sought to improve the therapeutic effect of MC *via* the development of MC-loaded PEG–PLGA micelles (MCPP-Ms) before they were developed into an *in situ* thermosensitive MC-loaded gel (MCPP-M-gel) for the treatment of SCI. Thus, this work sought to provide new ideas for the development and utilization of MC.

Materials and methods

Materials

Sinopharm Chemical Reagent Co., Ltd., supplied acetonitrile, ethanol, methanol, potassium chloride, ammonium acetate, P188 and P407. The phosphate buffer saline (PBS), sodium chloride, para-formaldehyde, 2% phosphotungstic acid and hematoxylin–eosin (HE) staining kit were provided by Beijing Solarbio Technology Co., Ltd. The minocycline (99% purity), glucan gel G-50, coumarin 6 and ethylenediaminetetraacetic acid disodium salt (EDTA-2Na) were purchased from Sigma-Aldrich (St. Louis, MO, USA). PEG3000–PLGA3000 was provided by Toyongbio (Shanghai, China).

Analytical method for determining MC content

To detect the MC content, a high-performance liquid chromatographic (HPLC) technique was employed, which was mainly composed of a Waters Symmetry C18 (5 μm, 4.6 mm × 250 mm) column with the eluent being buffer solution of ammonium acetate (obtained *via* dissolution of ammonium acetate-15 g, potassium chloride-10 g and ethylenediamine tetraacetate-5 g prior to dilution to 1000 mL) and acetonitrile at a ratio of 70 : 30. Other chromatographic conditions for the analysis were detection wavelength (280 nm), column temperature (25 °C), flow rate (1.0 mL min^{-1}) and injection volume (20 μL). The establishment of an *in vitro* MC standard curve showed a good linear relationship at a concentration range of 5–100 μg mL^{-1} with the following linear equation:

$$y = 22910x - 131687 \quad (1)$$

($R^2 = 0.9970$, where y denotes peak area and x represents MC concentration). The retention time for MC was 5.5 min (Fig. 1A).

Preparation of MCPP-M

Based on previous studies,[44] the thin film hydration method was used to prepare blank micelles and MCPP-M (PEG3000–PLGA3000 50 : 50). Through preliminary studies, the drug loading proportion was determined based on investigations of particle size and polydispersed index (PDI) of the micelles with different drug contents. Based on preliminary studies (data not shown), different ratios of MC : PEG–PLGA were investigated: 1 : 8, 1 : 9, 1 : 10, 1 : 11 and 1 : 12 (Table 1). Besides, a blank micelle was prepared with a particle size of 43 nm and a polydispersed index (PDI) of 0.217.

To prepare MCPP-M, MC and PEG–PLGA were accurately weighed into a round glass bottle before 30 mL of chromatographic ethanol was added to dissolve the mixture completely. Afterward, the bottle containing the solution was rotated to evaporate at 45 °C until a uniform thin film was formed. Under reduced pressure, rotavap was employed for 12 h to remove the residual organic solvent. Later, 10 mL of purified water was added to hydrate the film and allowed to stand for 20 min before it was filtered through 0.45 μm membrane filters to remove impurities and obtain MCPP-M. Notably, the best preparation was selected using the particle size, PDI and encapsulation rate.

Characterization of MCPP-M

NanoBrook 90 Plus particle size analyzer equipped with dynamic light-scattering (DLS) and phase-analysis light-scattering (PALS) techniques were employed to accordingly measure the zeta potential, particle size and PDI of MCPP-M based on existing method and conditions.[45] Specifically, the MCPP-M was appropriately diluted before measurement (in triplicate) of the above-mentioned physical characteristics at a 90° angle and temperature of 25 °C.

Morphological observation of MCPP-M using the transmission electron microscopic (TEM) technique

Observation of the morphology of MCPP-M was carried out after dilution of the sample to approximately 200 μg mL^{-1} with deionized water. Later, one drop of dried sample was placed on a copper net prior to staining with 2% phosphotungstic acid, and subsequent detection with TEM.

Estimation of encapsulation rate and drug loading of MCPP-M

Based on a modified existing method,[46] the encapsulation rate and drug loading of MCPP-M were detected after the separation of the micellar system with glucan gel chromatography. Briefly, the glucan gel G-50 (50 g) was placed into the chromatography column before the water balance. Afterward, the micelle (1 mg mL^{-1}) was carefully added to the column and eluted with purified water. Later, the sample (10 mL each) was collected before the content of the encapsulated MC was detected with HPLC. When MC could no longer be detected in the eluted purified water portion, a 0.2% sodium chloride solution was used for the detection of MC, which was considered the unencapsulated MC. In addition, the drug loading was measured through the following procedure: a certain concentration (1 mg mL^{-1}) of MCPP-M was placed in a tube and centrifuged for 30 min at 3700 rpm before the supernatant was removed and analyzed with HPLC. The calculation of the encapsulation rate

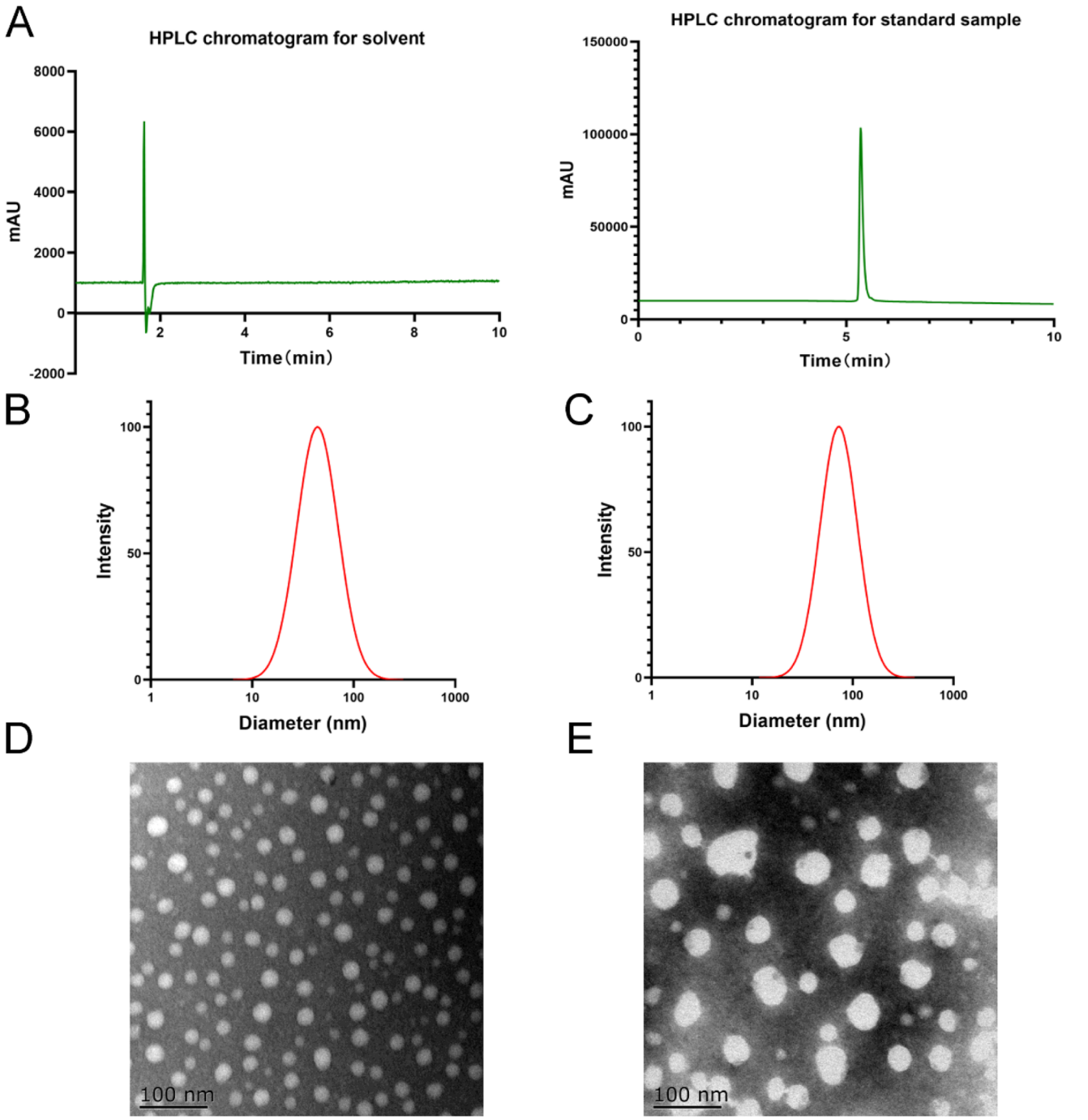

Fig. 1 Chromatographic analysis of minocycline (MC) and physical characterization of MC-loaded micelles (MCPP-M). (A) HPLC chromatogram for MC. Particle size distribution of (B) blank micelles and (C) MCPP-M. TEM micrographs of (D) blank micelles and (E) MCPP-M.

Table 1 Characteristics of different preparations of minocycline (MC) micelles ($n = 3$, mean ± standard deviation)

Ratios	Particle size (nm)	Polydispersed index (PDI)	Encapsulation rate (%)
1 : 8	162.32 ± 1.520	0.302 ± 0.006	63.21 ± 2.780
1 : 9	129.11 ± 2.050	0.283 ± 0.008	72.39 ± 2.190
1 : 10	72.16 ± 1.060	0.227 ± 0.005	89.38 ± 1.840
1 : 11	61.83 ± 1.080	0.221 ± 0.006	90.18 ± 2.010
1 : 12	59.81 ± 1.290	0.219 ± 0.004	91.65 ± 1.150

Table 2 Stability of MCPP-M after storage for 30 days at 4 °C and 25 °C ($n = 3$, mean ± standard deviation)

	PDI		Zeta potential (mV)		Particle size (nm)	
Period	4 °C	25 °C	4 °C	25 °C	4 °C	25 °C
0 day	0.227 ± 0.005	0.227 ± 0.005	−28.31 ± 0.900	−28.31 ± 0.900	72.16 ± 1.060	72.18 ± 1.140
15 days	0.229 ± 0.006	0.229 ± 0.008	−28.16 ± 0.930	−27.09 ± 0.970	73.12 ± 1.250	74.29 ± 1.610
30 days	0.229 ± 0.007	0.232 ± 0.009	−27.46 ± 0.980	−26.62 ± 1.120	73.68 ± 1.850	76.47 ± 1.950

and drug loading was based on the following existing eqn (2) and (3):[46]

$$\text{Encapsulation rate } (\%) = \frac{Q_{\text{encapsulated}}}{Q_{\text{total}}} \times 100\%, \quad (2)$$

$$\text{Drug loading } (\%) = \frac{Q_{\text{encapsulated}}}{Q_{\text{lipids}}} \times 100\%, \quad (3)$$

where $Q_{\text{encapsulated}}$ denotes the quantity of MC encapsulated in the micelle, Q_{lipids} denotes the total quantity of lipid content in the micelle and Q_{total} represents the total quantity of drug in the dispersed micelle.

Testing the storage stability of MCPP-M

Based on a modified method in a previous study,[47] the prepared MCPP-Ms were kept in a closed container at 25 °C and 4 °C for one month, wherein the micelle was sampled on days 0, 15 and 30 within the period to observe the physical appearance, while the particle size distribution, PDI and zeta potential were determined to test the stability of the formulation.

Testing the *in vitro* release profile of MCPP-M

Testing the *in vitro* release behavior of unencapsulated MC and MCPP-M was performed using dialysis method[48] with three buffer solutions [PBS (pH 7.4 and 6.8) and hydrochloric acid (HCl, pH 1.2)] as release media. Afterward, an aliquot (1 mg) of MC (solubilized in a very small amount of methanol) and MCPP-M (dissolved in 1 mL of purified water) were placed in a dialysis bag (MV = 3500 dalton). After the two ends of the dialysis bags had been tied, the bags were placed in an Erlenmeyer flask containing 100 mL of the release media prior to oscillation (at 37 °C, 100 rpm). Afterward, samples (1 mL each) were collected at pre-determined intervals (10, 30, 45, 60, 90, 120, 180, 240, 360, 480, 600, 720, 1440, 2160, 2880, 3600 and 4320 min), while 1 mL of fresh release media were added simultaneously. Later, the samples were diluted with methanol in accordance with the HPLC method described above. The cumulative MC release was carried out while considering the replenishment of the media,[49] and the entire measurements were performed in triplicate prior to the calculation of the average MC concentration.

Uptake of MCPP-M by neural-crest-derived ectoderm mesenchymal stem cells (EMSCs)

A previously developed fluorescence microscopic technique[50] was utilized to ascertain the uptake of MCPP-M by the EMSC cells. In brief, the EMSCs were seeded at 1×10^5 cells per well density on coverslips in Dulbecco's Modified-Eagle's Medium (DMEM, Wisent Biotech., Co., Ltd., Nanjing, China). After they had grown 70% confluence, the medium was replaced with a fresh medium composed of FITC labeled BCPP-M at a final MC concentration of 10 μg mL^{-1} before incubation at various times (1, 2, 4 and 8 h). Later, PBS was used to wash the cells twice before fixing them with para-formaldehyde (PFA, 4%) and subsequent staining of the nucleus for 5 min with 4′,6-diamidino-2-phenyl-indole (DAPI, 0.5 μg mL^{-1}) in the dark at room temperature. The cells were observed with a fluorescence microscope (Labophot-2, Nikon, Melville-NY, USA) after the coverslips had been mounted on a glass slide.

Preparation and characterization of MCPP-M-gel

The MCPP-M-gel was prepared using the method described in a previous study[41] with slight modifications. Concisely, 5 mL of MC–PEG–PLGA was accurately weighed in water (10 mg mL^{-1}). It was then poured into test tubes pre-supplemented with 0.18 g of P188, 0.54 g of P407 and 1 mL of 0.003 g per mL chitosan glacial acetic acid solution. After complete mixing, the mixture was naturally expanded at 4 °C and stored overnight to remove air bubbles, after which a transparent solution was formed to obtain the MCPP-M-gel. Notably, the above procedure was followed to prepare a blank micellar thermosensitive gel that did not contain MC.

Morphological observation of MCPP-M-gel using the scanning electron microscopic (SEM) technique

As described elsewhere,[41] a dehydrated MCPP-M-gel was lyophilized before observation of the morphology with SEM (S-3400, Hitachi, Japan) after the gel was coated with gold. Both MCPP-M-gel and blank thermosensitive gel were visualized using the appropriate technique.

Determination of gel formation temperature (GFT) and gelation time (GT) of MCPP-M-gel

The inverted test tube method[51] was employed to determine the GFT of the MCPP-M-gel. In brief, an appropriate volume of MCPP-M-gel was placed in the transparent tube. The sample was placed under a constant temperature water bath and subjected to slow heating starting from 30 °C at a temperature amplitude of 1 °C, coupled with temperature insulation of 10 min. Later, the tube was inverted, and the flow of the gel was observed to determine whether the gel was formed. Afterward, the gel was removed and placed in a 4 °C refrigerator. After the sol was

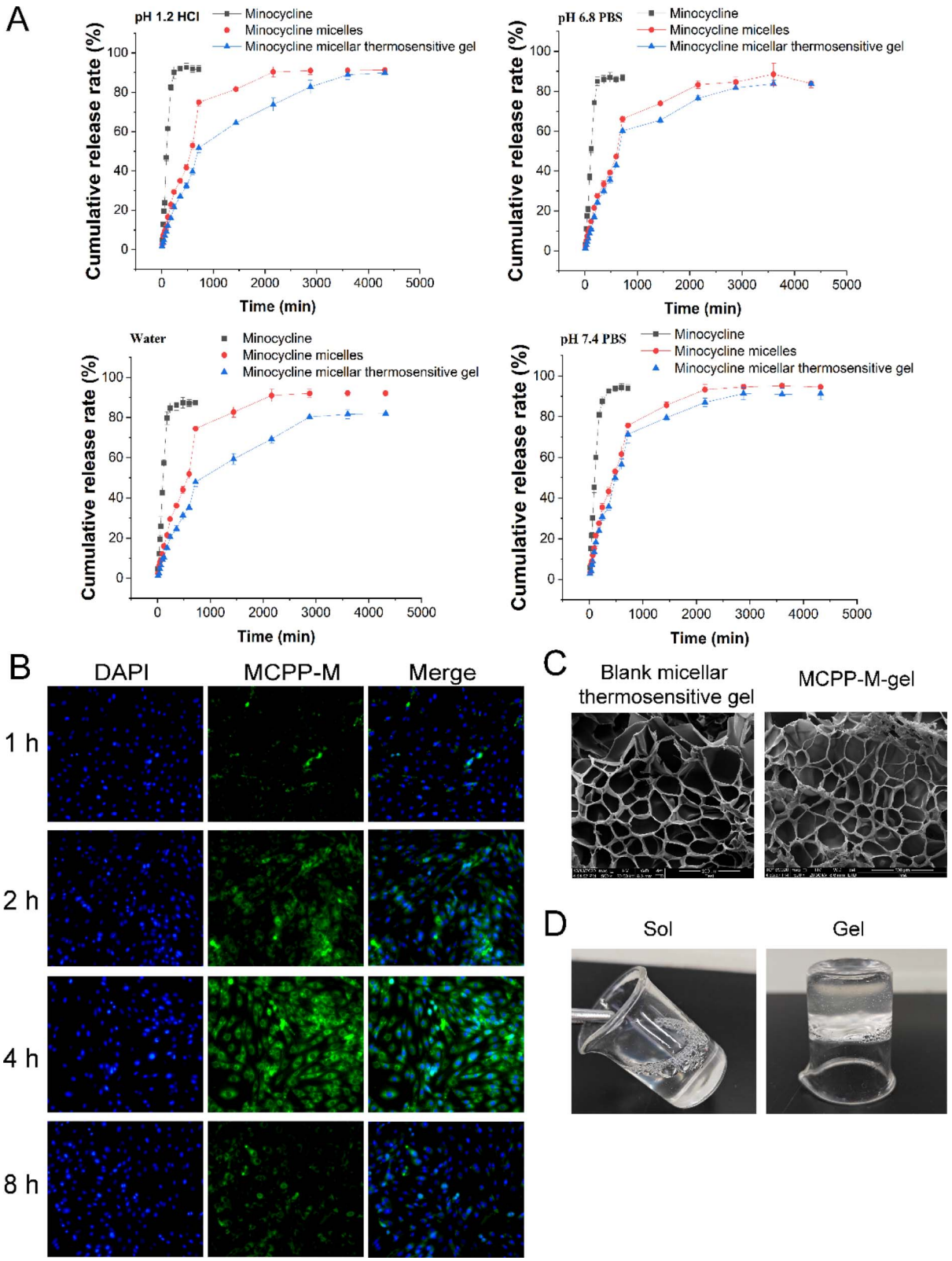

Fig. 2 Physical characterization of MCPP-M and MC-micellar thermosensitive hydrogel (MCPP-M-gel). (A) *In vitro* release of MC from free MC, MCPP-M and MCPP-M-gel. (B) Effect of MCPP-M uptake by neural-crest-derived ectoderm mesenchymal stem cells (EMSCs) (20×). (C) SEM micrograph of blank micellar thermosensitive gel and MCPP-M-gel. (D) Digital photos of MCPP-M-gel changed from sol to gel.

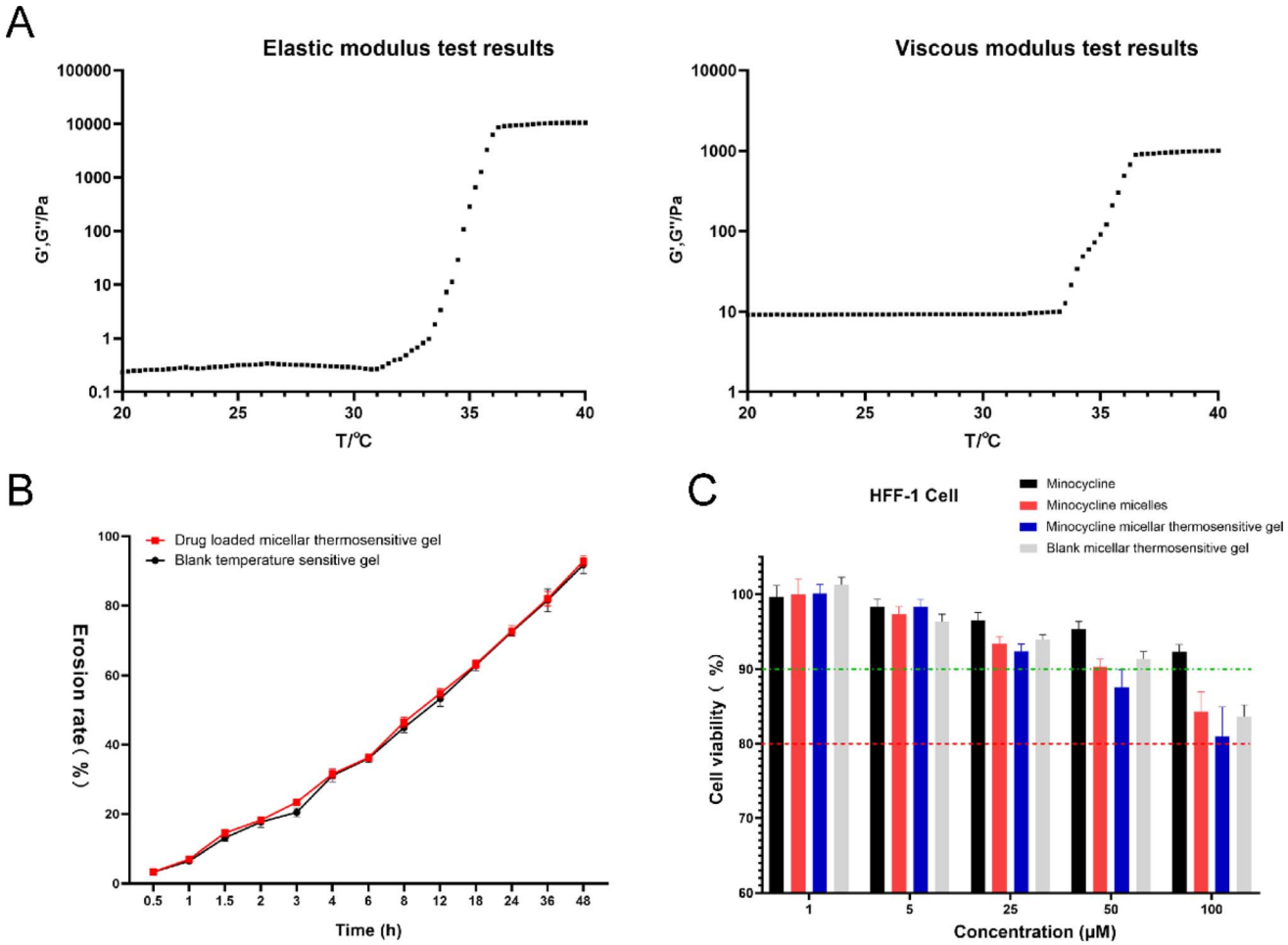

Fig. 3 Minocycline (MC)-loaded micellar thermosensitive hydrogel (MCPP-M-gel) characterization. (A) Elastic and viscous moduli of MCPP-M-gel. (B) Erosion rate of MCPP-M-gel. (C) Biosafety of MCPP-M-gel.

restored, the gel was placed in a water bath. Later, the heating interval was narrowed, and the gel temperature (T_g) was accurately determined after estimating the approximate gel temperature. This procedure was repeated three times, and the average was calculated.

Regarding the measurement of GT, a procedure described in previous works[51,52] was employed. Briefly, the transparent tube filled with 2 mL of MCPP-M-gel was placed in a 37 °C constant temperature water bath to observe a change in the mixture. When the colorimetric tube was inverted and the solution was no longer flowing, the solution was considered to form a hydrogel.

Determination of erosion rate and rheological profile of MCPP-M-gel

The *in vitro* erosion rate of MCPP-M-gel was determined at 37 °C using a membrane-free system, as stated elsewhere.[53] The empty bottle (10 mL cillin bottle) was weighed, and MCPP-M-gel (about 2 g) was added before placement in a mechanical shaker (37 °C, 150 cycles per min) for 10 min so that the polymer solution could completely form the gel. Afterwards, the gel was removed, and 1 mL of PBS (pH 7.4) was added as the release medium before the sample was placed into a water bath with a constant temperature oscillator, which oscillated at 37 °C and a rate of 30 rpm. Later, the release medium was completely discarded at the set time, and the bottle was dried prior to weighing. Then, the water bath was equilibrated for 10 min and supplemented with 1 mL of PBS solution (37 °C). This procedure was repeated until the remaining gel was less than 10% of the starting amount. Three parallel groups were set for each experiment. Then, erosion times were recorded, and the average was calculated.

To determine the rheological profile of the MCPP-M-gel, a strain-controlled rheometer was utilized for the experiment. The apparatus utilized the parallel plate method, wherein the diameter was roughly 25 mm, whereas a space of 1.00 mm was maintained between the parallel and Peltier plates. Later, a frequency sweep test was employed to determine the elastic modulus (G') and viscous modulus (G''). At a rate of 1 °C min^{-1}, the plate was heated from 10 °C to 45 °C while maintaining the frequency at 10 rad s^{-1}. Afterward, the sol or gel behavior was evaluated as $G' < G''$ (sol) or $G'' < G'$ (gel) of the hydrogel system.

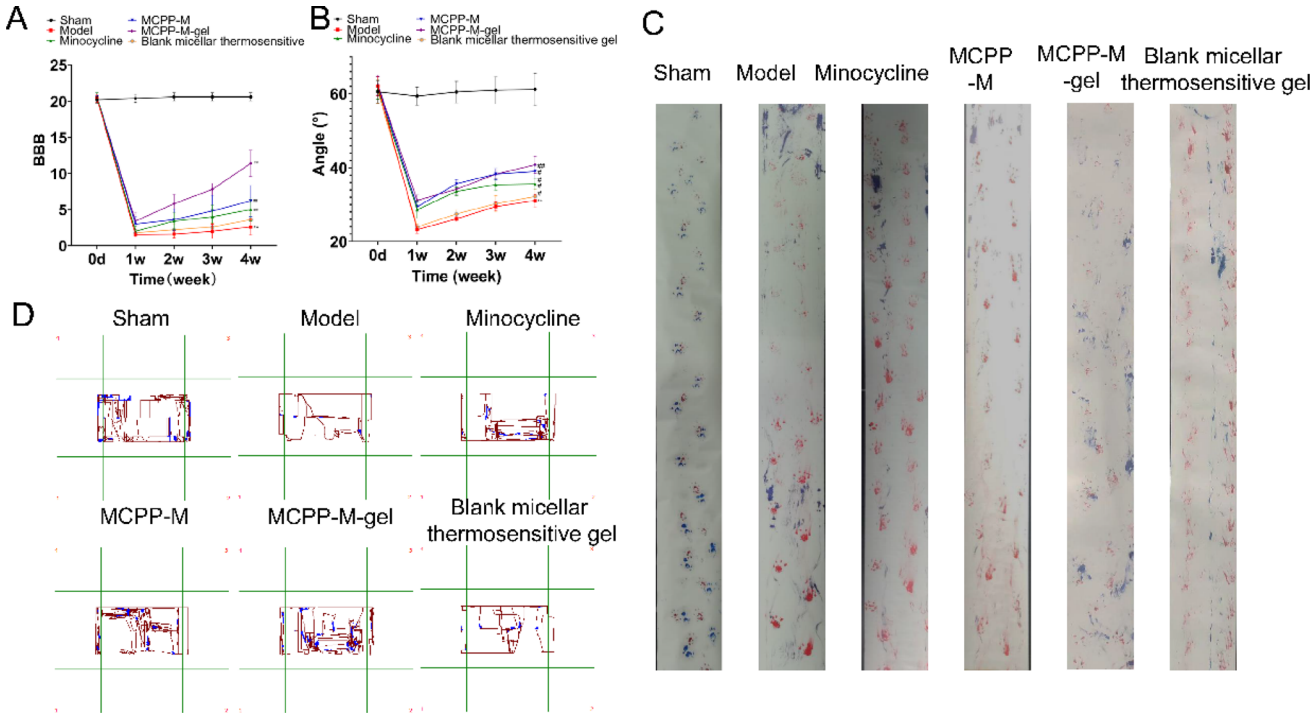

Fig. 4 Functional behavior assessment. (A) BBB score. (B) Slanted-plate experiment. (C) Foot-print inspection. (D) Open field experiment.

Testing of MCPP-M-gel effect on cell viability

Prior to their use in cytotoxicity studies, the Chinese Academy of Sciences Stem Cell Bank benevolently supplied human foreskin fibroblast cells (HFF-1), which were cultured based on ideas from previous studies.[54] Concisely, culturing of the cells under appropriate conditions (37 °C and 5% CO_2) was performed with DMEM (Wisent Biotech., Co., Ltd., Nanjing, China) comprising penicillin–streptomycin (PS, 1%, Gibco, Thermo-Fisher Scientific, Waltham, MA, USA) and fetal-bovine serum (FBS, 15% heat inactivated, Bioagrio, Mountain View, CA, USA). Only cultured cells that had reached the lag growth stage were used for the experiment. The cells were seeded into 96 well plates (100 μL per

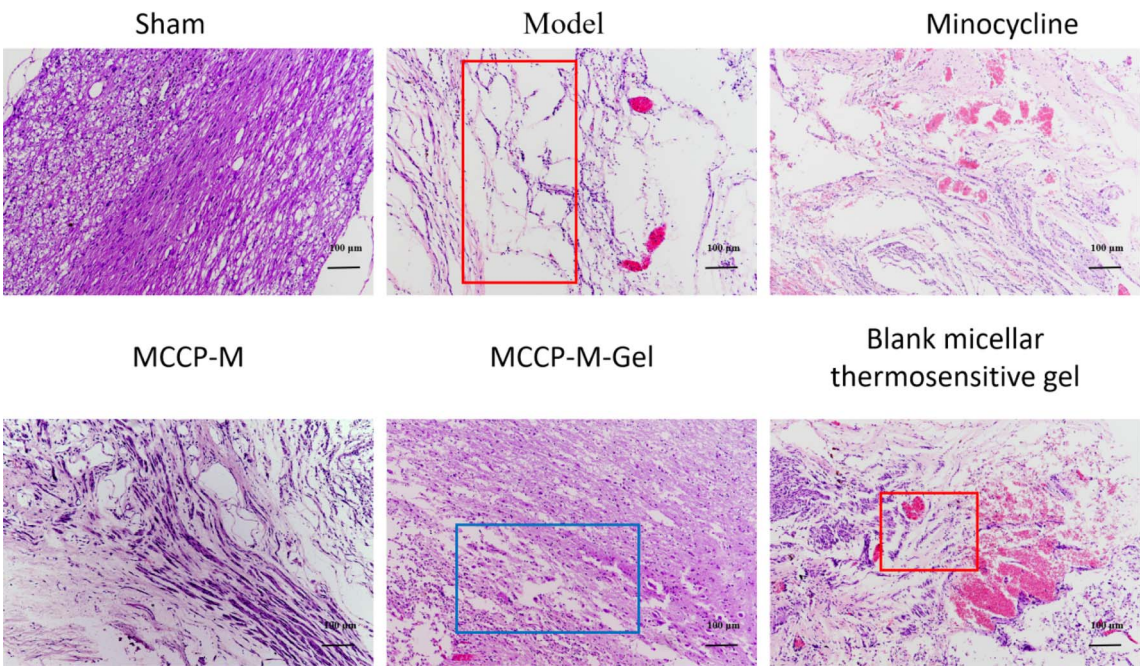

Fig. 5 Histopathological observation (10×).

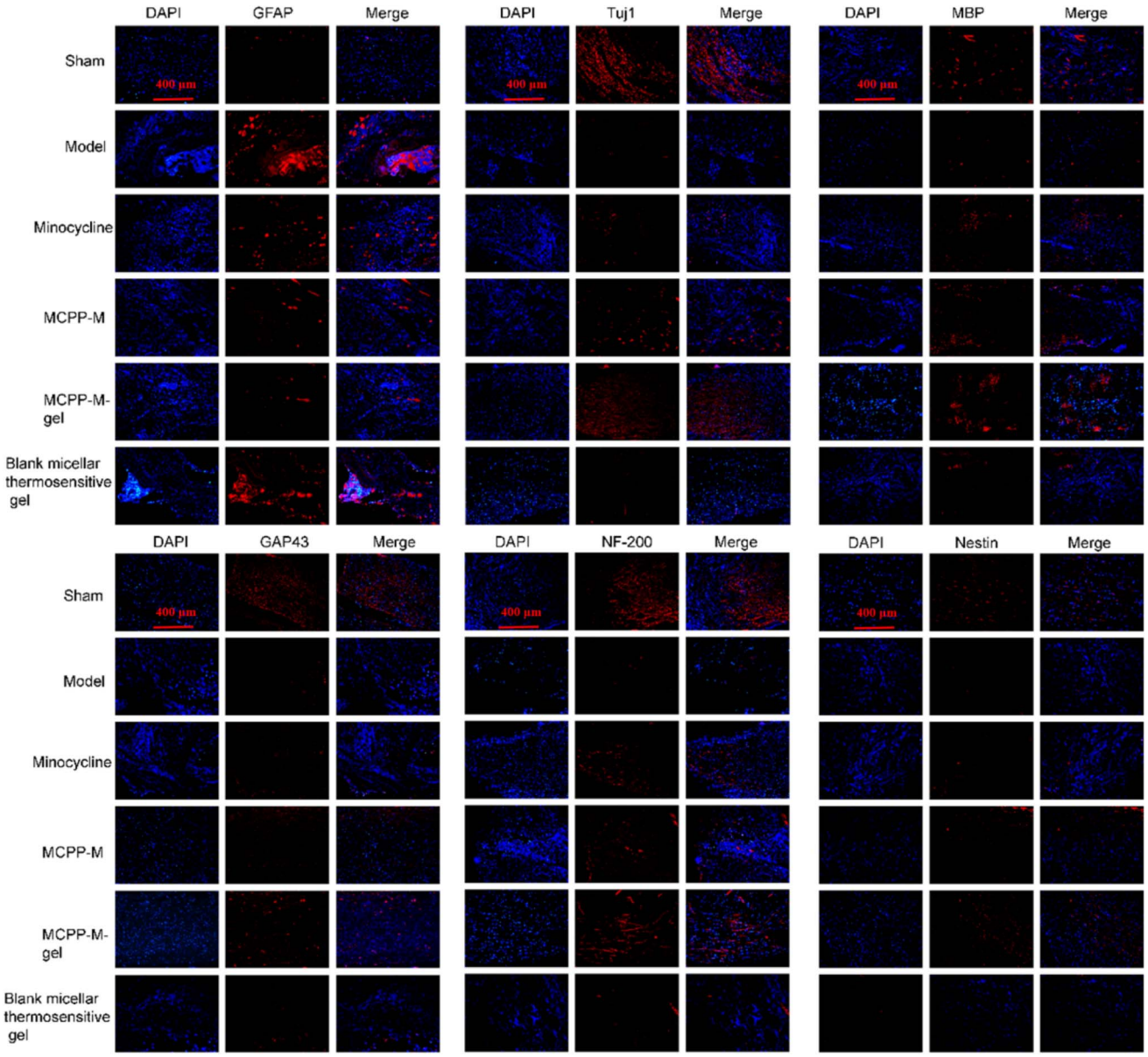

Fig. 6 Expressions of GFAP, Tuj1, MBP, GAP43, NF-200, and nestin proteins were detected using immunofluorescence assessment (10×).

well) under conditions such as density (3×10^5 cells per well) and medium per well (2 μL) before incubation under the same above-mentioned conditions. The following four groups were studied: MC, MCPP-M, MCPP-M-gel and blank micellar thermosensitive gel. Using 3-[4,5-dimethyl-thiazol-2-yl]-2,5-diphenyl-tetrazolium bromide (MTT) assay, the cells were co-cultured with varied concentrations (1, 5, 25, 50 and 100 μM) of the above-mentioned dosage forms. Subsequently, incubation was performed for 1–4 h under the same aforementioned conditions after the addition of MTT solution (10 μL) to each well of the above-mentioned plate. For each experiment, at least five replicates were set up for each group. Before measuring the absorbance at 570 nm with a microplate reader, the crystals of formazan were dissolved in a solubilization solution (dimethyl sulfoxide). Later, cell viability was calculated based on an existing equation.[55]

Testing of the *in vitro* release behavior of MCPP-M-gel

In testing for the *in vitro* release behavior of MCPP-M- gel, the same method, releasing media, conditions, apparatus and procedures were employed as described above for MCPP-M.

Surgery of rats for construction of SCI model and administration of MCPP-M-gel

The Sprague-Dawley (SD) rats (with an average weight of about 250 g) were supplied by the Center for Laboratory Animal Research at Jiangsu University (Zhenjiang, China). The rats fasted the night before the surgery, and they were not given

water on the surgery day. After ensuring that the animals were well cared for in a conducive laboratory environment, approval was obtained for the animal experimental protocol from the Jiangsu University Ethics Committee for the Care and Use of Laboratory Animals (UJS-IACUC-2023040801). The operative surgery was performed as described elsewhere[56] with slight modifications. In short, 7% chloral hydrate was employed for the anesthesia of the rats after disinfection of the back skin of the animal *via* the intraperitoneal route. Subsequently, the rats were placed on an ultra-clean table for the operation process, particularly by positioning the T12 vertebrae (located in the rat of the highest point) after the midline back incision. Later, the rats were opened layer by layer, and the muscles and vertebrae were separated before forceps were used to remove the spine and dura to expose the bone marrow. Ultimately, blade transection was performed at the T10–11 segment spinal cord to cause complete spinal cord transection.

The following groups (n = 10 rats in each group) were analyzed: group A (sham rats), group B (model rats), group C (rats that received MC), group D (rats that received MCPP-M), group E (rats that received MCPP-M-gel) and group F (rats that received blank micellar thermosensitive gel). Treatment was carried out as follows. Rats in groups C, D, E and F received their respective dosage forms at a dose of 90 mg kg^{-1} (ref. 57) once daily for 1 week *via* intra-peritoneal injection, followed by the application of MCPP-M-gel and blank micellar thermosensitive gel to the injury site of SC; subsequently, a layer by layer closure of the muscles and skin was performed. The rats were subjected to good post-operative care, as established in other works.[58]

Post-injury motor behavior assessment *via* open field evaluation

Open field motor function at 0, 3, 7, 14, 21 and 28 days was assessed using the Basso, Beattie and Bresnahan (BBB) scoring methods.[59] Each hindlimb was sorted by two blind observers and simultaneously videotaped. The BBB score ranged from 0 (unchanged hind limbs) to 21 (normal gait) to assess functional improvement after injury and treatment. Later, BBB was performed in uninjured animals to determine whether these materials had any early impairment of normal motor function. Through the test device, the slope test was performed at 0, 3, 7, 14, 21 and 28 days. The maximum angle of the rats holding the posture for 5 s without falling was recorded and averaged to obtain a single score for each animal.

Behavioral investigation

All the rats were subjected to a series of behavioral analyses after sciatic nerve injury. Restoration of locomotor activity in the left hind limb was considered evidence of adequate regeneration of muscle and recovery of function after sciatic nerve injury, which was monitored by analyzing the pattern of free walking using the method referenced in previous studies.[60] In this test, the rats were placed on a track (500 mm long, 100 mm wide, covered with white paper at the bottom and placed in a black box). Meanwhile, they were allowed to walk with dark dye on the soles of the hind paw before the analysis of their gait and recovery.

Histological evaluation

After 28 days, the histological observation was performed after the preparation of appropriate solutions, namely sodium pentobarbital (4 mg/100 g body weight), sodium chloride (0.9%), and paraformaldehyde (PFA, 4%, 0.0 1 M) that was buffered with PBS (pH = 7.4). Later, SC was collected from T8–T10 before the sample was fixed in PFA (4%) and embedded in paraffin. Afterward, hematoxylin–eosin (HE) staining was carried out, and the lesion center was observed under a light microscope.

Detection of relevant protein expression using immunofluorescence techniques

A previously established method[61] was followed to perform immunofluorescence techniques.

In performing the immunofluorescent technique, the SC sections were treated overnight with primary antibodies, namely Tuj1 (1 : 100, Abcam, Cambridge, England), GAP43 (1 : 100, Abcam, Cambridge, England), GFAP (1 : 100, Abcam, Cambridge, England), NF-200 (1 : 100, Cell Signaling Technology, USA), MBP (1 : 100, Abcam, Cambridge, England) and nestin (1 : 100, Abcam, Cambridge, England), at 4 °C before incubation at 37 °C for 2 h with HRP-conjugated secondary antibodies. Prior to the observation of the SC sections using the fluorescent microscopic technique (Eclipse 80i, Nikon, Japan), the sections were stained using an Immunol Fluorescence Staining Kit (Beyotime, China).

Statistical analysis

Statistical analysis and construction of the experimental data into graphs were performed with Graph-Pad Prism v8.0 software (USA). Comparison between two groups was carried out using an unpaired t test, while more than two groups were compared using a one-way analysis of variance (ANOVA). In terms of statistical significance level, at least $p < 0.05$ was considered after the data were expressed as mean ± standard deviation.

Results and discussion

Preparation and physical characterization of MCPP-M-gel

The MCPP-M-gel was successfully prepared using the thin film hydration method, as described in the methods. During the preparation of MCPP-M, different ratios of MC : PEG-PGLA co-polymer (Table 1) were explored. From Table 1, the physical characteristics of the above-mentioned ratios (1 : 8 to 1 : 12) ranged from 59.81 ± 1.29 to 162.32 ± 1.52 nm (particle size), 0.219 ± 0.04 to 0.302 ± 0.01 (PDI) and 63.21 ± 2.78 to 91.65 ± 1.15% (encapsulation rate). It was observed that the particle size and PDI of the micelle decreased, while the encapsulation rate increased with an increase in the concentration of the PEG-PGLA co-polymer. Based on the stability of MCPP-M, a formulation with an MC : PEG-PGLA ratio of 1 : 10 was selected for subsequent studies. The preparation had a relatively smaller size coupled

with a high zeta potential and encapsulation rate. In comparison with blank micelles (particle size of 43 ± 0.11 nm and a PDI of 0.217), the MCPP-M had a micellar size of 72.16 ± 1.060 nm, PDI of 0.227 ± 0.005, zeta potential of −28.31 ± 0.900 mV, encapsulation rate of 89.38 ± 1.840% and drug loading of 8.08 ± 0.08%. The observed smaller hydrodynamic diameter of blank micelles than MCPP-M may be owing to the incorporation of a large drug molecule such as MC (457.48 g mol^{-1}) within the micellar core.[62] However, the structure of the MCPP-M-gel will be comprehensively investigated in the future to potentially understand the actual structure of the hydrogel. Besides, the negative sign of the zeta potential of MCPP-M may be ascribed to free carboxylic ends of PLGA moiety in the co-polymer.[63]

Further, MCPP-M displayed increased loading of MC, which may be attributed to its high lipophilic nature. Usually, hydrophobic drugs, such as MC, favorably interact with the lipophilic moiety of PEG-PGLA polymers, thereby increasing the loading efficiency of such drugs. Additionally, the encapsulation rate of MCPP-M may be increased by the bulky nature of the PEG-PGLA polymer[64] *via* reduction of net sheer stress induced by increased particle size after MC incorporation.[65] In terms of micellar morphology, MCPP-M particles were observed to be spherically distributed with any sign of agglomeration, which relatively agreed with that of blank micelles. Collectively, MCPP-M exhibited reasonably increased zeta potential and encapsulation rate, which are important attributes for the subsequent development of the hydrogel.

Storage stability and *in vitro* release profile of MCPP-M

Because micelles tend to disintegrate and release entrapped drugs prematurely, this phenomenon can decrease the efficiency of drug delivery and potentially create concerns about toxicity.[66] Therefore, it is essential that the excipients of the preparation contribute immensely to the stability of the micelles. As described in the methodology, the stability of MCPP-M was investigated for 30 days at 4 °C and 25 °C. The results are depicted in Table 2. Physical characteristics such as PDI, zeta potential and particle size of MCPP-M were evaluated, which were found to be stable throughout the studied period. Although these characteristics altered slightly, they did not reach a statistically significant level. Thus, the developed MCPP-M demonstrated appropriate stability, which is essential for *in vivo* application. It is possible that the stability of MCPP-M may be due to the PEG-PGLA polymer,[67] which has previously been used to stabilize lipophilic molecules, such as MC.

To simulate the *in vivo* environment, we investigated the *in vitro* release pattern of MC from MCPP-M using the diffusion technique. Fig. 2 shows the result of the *in vitro* cumulative release profile of MCPP-M. Compared to free MC (Fig. 2A), the cumulative MC release from MCPP-M at 72 h demonstrated a prolonged release pattern (Fig. 2A). In particular, at 12 h, free MC released the drug at significantly increased cumulative rates in all the four media compared to MCPP-M [HCl pH 1.2 (95.52 ± 2.00% *vs.* 77.94 ± 2.00%, $p = 0.0011$), PBS pH 6.8 (86.64 ± 1.55% *vs.* 66.21 ± 1.64%, $p = 0.0001$), water (87.47 ± 1.98% *vs.* 74.46 ± 2.81%, $p = 0.0028$) and PBS pH 7.4 (94.01 ± 1.71% *vs.* 75.65 ± 3.51%)]. The observed fast release rate of MC within 12 h corroborated previous studies.[68] This phenomenon may be attributed to the increased solubility of MC in an aqueous medium.[69] Beyond 12 h, the amount of MC released from free MC could not be detected in the four media. However, MCPP-M released MC in a sustained-release manner until 72 h, wherein maximum cumulative release rates in the four media were achieved in an order of PBS pH 7.4 (94.55 ± 1.48%) > water (92.07 ± 1.25%) > HCl pH 1.2 (91.25 ± 0.90%) > PBS pH 6.8 (83.93 ± 2.14%). Overall, the *in vitro* release of MC was prolonged by the micellar system for 72 h, which may have improved the delivery of the drug to the injured area of the SC.

Uptake of MCPP-M by EMSCs

A fluorescence microscopic technique was employed to ascertain the potential absorption of MCPP-M *in vitro*, wherein the micelles were labeled with green-fluorescent FITC dye before incubation with EMSCs. From the results displayed in Fig. 2B, at 1 h, the MCPP-M could be observed to accumulate in the nuclei (as indicated *via* blue DAPI dye) of EMSCs. However, MCPP-M labeled with FITC was taken up by macrophages and the cytoplasm of EMSCs began after 2 h of incubation. Later, nearly all MCPP-M could be taken up by EMSCs after 4 h of incubation but subsequently declined after 8 h. This phenomenon may be attributed to the transport of MCPP-M into other endocytic intermediates in EMSCs.[70] Collectively, these findings suggest the rapid internalization of MCPP-M by EMSCs *via* the effective intrinsic action of the cell. The effect of the physical characteristics of MCPP-M on cellular uptake and the mechanism underlying the uptake of the micelles by EMSCs was not studied in this work. Because these parameters are important for scientists to understand the targeted delivery behavior of MCPP-M, our subsequent research work will prioritize this limitation.

Preparation, gelation characteristics and erosion rate of thermosensitive MCPP-M-gel

Based on the challenges of micelles, a thermosensitive micellar hydrogel of MC was prepared and characterized. After the successful development of the thermosensitive MCPP-M-gel, its transformation from sol to gel was observed using the inverted test tube method. Through SEM micrographs of the cross-section of the lyophilized MCPP-M-gel, an irregular microporous structure of the gel (Fig. 2C) was observed. In terms of gelation formation, it was discovered that after the MCPP-M-gel was heated (to 37 °C), it changed from sol to gel (Fig. 2D). In contrast, MCPP-M-gel changed from gel to sol after the temperature decreased to room temperature (25 °C). Additionally, the GFT and GT of MCPP-M-gel were determined to be 35.13 ± 0.31 °C and 101.77 ± 3.95 s, respectively. Because the average GFT of MCPP-M-gel was closer to the physiological temperature (37 °C), this suggests that the hydrogel could potentially be transformed from sol to gel under physiological conditions after injection. A rheological test was employed to further affirm the transformation of MCPP-M-gel from sol to gel. As illustrated in Fig. 3A, increased elastic modulus (G', G'') and viscous modulus (G', G'') were observed after the

temperature had risen to approximately 35 °C. Both elastic and viscous modulus were similar, indicating that the phase-transition temperature of the MCPP-M-gel was around 35 °C. Overall, these results imply that MCPP-M-gel demonstrated thermally reversible behavior. Moreover, the erosion rate for 48 h was determined. The results are displayed in Fig. 3B. The erosion rate usually entails depletion of the polymeric material, which, in this case, was PEG-PGLA co-polymers. It was observed that blank micellar thermosensitive gel and MCPP-M-gel eroded gradually and increased over time, achieving a maximum rate (92.84%) at 48 h (Fig. 3B). Overall, these findings suggest the successful preparation of MCPP-M-gel, which demonstrates acceptable physico-mechanical properties.

Biosafety and *in vitro* release of MCPP-M-gel

Cell death degree and cell proliferation suppression after chemical exposure are measured through cytotoxicity assays. Because novel nanoparticles are to be applied clinically, it is relevant to determine their cytotoxic effects on the biological environment. In this regard, the cytotoxic effects of four dosage forms (namely MC, MCPP-M, MCPP-M-gel and blank micellar thermosensitive gel) were ascertained *in vitro* using HFF-1 cells. Fig. 3C depicts the effects of MC, MCPP-M, MCPP-M-gel and blank micellar thermosensitive gel on HFF-1 cell viability. It was observed that the cell viability of HFF-1 decreased as the concentration of the dosage forms increased. At higher concentrations (50 μM) of the dosage forms, the cell viability of HFF-1 was still above 80%, suggesting that the above-mentioned dosage forms were biocompatible, and hence can potentially be applied in the clinical settings.[71] The *in vitro* study of the dosage forms provides only a rapid generation of knowledge on their biosafety. This investigation lacks an *in vivo* toxicological outcome, which is very crucial for the validation of the formulations. Despite this limitation, *in vitro* biosafety results can be employed as predictors prior to the validation phase of toxicological evaluation. In the not-too-distant future, our group will comprehensively investigate the mechanism underlying the interaction of the above-mentioned dosage forms with biological systems.

The *in vitro* release profile of MC from MCPP-M-gel was also evaluated using the same method described for the micelle. In general, the MCPP-M-gel exhibited a prolonged release of MC. The release of the drug started as early as 10 min (approximately 3%) in all the media and continued until 72 h. The rates of cumulative release of MC from MCPP-M-gel in the four media at 72 h were in the following order: PBS pH 7.4 (91.25 ± 2.90%) > HCl pH 1.2 (89.86 ± 2.38%) > PBS pH 6.8 (83.81 ± 1.87%) > water (81.94 ± 2.07%). However, the difference between the total amount of MC released from MCPP-M (94.55 ± 1.48%) and MCPP-M-gel (91.25 ± 2.90%) was statistically insignificant, with the amount of the drug released by the former being slightly higher than that of the latter. This seeming difference may be owing to the potential of hydrogels to control the release of drugs in a prolonged fashion,[72] which has great prospects for possible clinical applications in the difficult-to-reach areas within the human body.

Effect of MCPP-M-gel on SCI

Treatment for complex SCI entails the regeneration of neurons and functional recovery. The prevention of neuronal cell death is usually a major aim of neuroprotection, which is achieved by restricting the processes of secondary injury that occur minutes, hours and days after the incidence of primary injury. Few successes have been achieved in using traditional treatment strategies for secondary injury in SCI. Hence, a novel approach to incorporating small molecules into biomaterials that have the potential to promote the long-lasting delivery of drugs and neuroprotection has the prospect of treating SCI. The MH system exhibits the above-mentioned characteristics very well. Hence, the MH system was utilized to incorporate a known neuroprotective agent, such as MC (MCPP-M-gel). Afterward, the potential of MCPP-M-gel to promote neuronal regeneration was evaluated in a rat's SCI model.

Effect of MCPP-M-gel on functional recovery from SCI

The BBB score and slanted-plate experiment were employed to measure functional recovery. Then, the effect of MC, MCPP-M, MCPP-M-gel and blank micellar thermosensitive gel on the functional recovery of SCI rats for four weeks was observed. Fig. 4A and B illustrate the therapeutic effect of MC, MCPP-M, MCPP-M-gel and blank micellar thermosensitive gel *via* BBB locomotion score and slanted-plated experiment, respectively. In terms of BBB scoring, there was a gradual increase in the BBB scores of the rats in each group throughout the 28 day post-SCI period. Notably, after 28 days, the rats that received MCPP-M-gel substantially attained a behavioral score of 11.4 compared to other groups: model (2.6), MC (5.0), MCPP-M (6.2) and blank micellar thermosensitive gel (3.6). The experimental inspection of rat foot-print presents rats' gradual movement ability between distinct groups and differences in trajectories of hind limbs (Fig. 4C) throughout the study periods after treatment. In this regard, it was observed that the rats in the sham group dragged and deflected their hind limbs. Through foot-print inspection, nearly consistent trajectories of the hind-limbs of rats were observed in the MCPP-M-gel groups, amid improvement in the extent of tripping and swaying, although the rats in each group struggled to support their weight for movement of their hind-limbs. The treatment effect of MCPP-M-gel may be ascribed to the long-lasting release of MC,[73] which may have promoted adequate regeneration of muscle and recovery of function after sciatic nerve injury.

Effect of MCPP-M-gel on neuronal regeneration

Histologically, the effect of MCPP-M-gel on neuronal protection through histopathological evaluation was observed using HE staining. The results of HE staining (Fig. 5) demonstrated divergences in terms of morphology within distinct groups. In particular, neuronal differences were observed. In the untreated groups, the SCI generally depicted tissues that were larger, hydrolysable, loosely structured, and coupled with neuronal and nuclear. Three days after SCI, it was observed that rats in the untreated group exhibited substantial shrinking of

morphology with the presence of disordered structures and increased reduction in neuronal numbers (as shown in the red boxes in Fig. 5 model and blank micellar thermosensitive gel). Importantly, the SCI of rats that received MCPP-M-gel displayed a significant reduction in the damaged area after 28 days of treatment, amid re-organization of the injured sites and neuronal retain (as shown in the blue boxes in Fig. 5 MCPP-M-gel). These results collectively suggest that MCPP-M-gel could promote neuronal regeneration at the injured site of the SC, which corroborates existing works.[74] It is possible that MCPP-M-gel was quickly transformed to hydrogels *in situ* under the physiological conditions at the injured site of the SC, which delivered MC in a sustained manner for improvement in the neuroprotective activity of MC.

Further confirmation of the neuroprotective potential of MCPP-M-gel was carried out by performing an immunofluorescence technique using markers, such as GFAP, Tuj1, MBP, GAP43, NF-200 and nestin (Fig. 6). As a marker of astroglial injury, GFAP is used to ascertain the incidence and severity of traumatic SCI. Additionally, Tuj1 is a neuronal marker for the identification of neural differentiation.[75] Similarly, MBP is considered a marker of injury to brain tissue; hence, it is used in the diagnosis of neurological diseases.[76] As a phosphoprotein of axons, the GAP43 is regarded as an indicator for the growth of axons and synapses, which is increasingly expressed during traumatic SCI.[77] Additionally, NF-200 can be used as an index of large alpha–beta fiber neurons that are myelinated.[78] Finally, nestin is a protein marker of neuroprogenitor, especially that of the hippocampus, which can be developed into astrocytes and neurons.[79] One way or the other, these proteins play an important role in neuronal regeneration. Hence, a potential neuroprotective agent, such as MCPP-M-gel, should potentially increase or lower its expression in SC tissues. Using the immunofluorescence technique, it was observed that MCPP-M-gel treatment and other dosage forms the up-regulated expression of Tuj1, MAP43, NF-200, MBP, GAP43 and nestin but the down-regulated expression of GFAP in SC tissues, while the hydrogel showed better effect.

This study did not conduct a more comprehensive evaluation of the biocompatibility and immunogenicity of MCPP-M-gel, as these characteristics may affect the tolerance and efficacy of the implant. Although cell toxicity tests were conducted in this experiment, the *in vitro* results may not be completely consistent with the *in vivo* situation, and further in-depth studies are required on the safety of MCPP-M-gel material. The materials used in this experiment were prepared on a laboratory scale, and the preparation process may be difficult to scale up to industrial production. Therefore, further optimization may be required in the production process to facilitate the clinical application of this technology. These are all areas that must be continuously improved in subsequent experiments.

Conclusions

Herein, a micellar thermosensitive MC-loaded hydrogel with PEG-PGLA co-polymer as the biomaterial (MCPP-M-gel) was successfully developed for the treatment of SCI. The MCPP-M-gel had acceptable physical characteristics, such as smaller particles, narrow PDI and increased encapsulation rate, and it sustainably released MC within 72 h. Evaluation of MCPP-M-gel through *in vivo* studies revealed that the hydrogel promoted neuroprotection and functional recovery in SCI rats by increasing the expression of Tuj1, MAP43, NF-200, MBP and nestin albeit reducing GFAP expression in damaged areas of SCI. Thus, the incorporation of MC into MCPP-M-gel may have potentially improved its neuroprotective effect in SCI rats.

Data availability

Data will be available upon request to the corresponding author.

Conflicts of interest

No competing interest declared by authors.

Acknowledgements

This project was supported by 2022 General Program of Jiangsu Provincial Health Commission (M2022026), 2022 Key Discipline Innovation Team of Wuxi Health Commission (CXTD2021022), General Program of Wuxi Health Commission (M202357) and Wuxi Health Commission project (Q202215).

References

1 Z. Nazemi, M. S. Nourbakhsh, S. Kiani, Y. Heydari, M. K. Ashtiani, H. Daemi and H. Baharvand, *J. Controlled Release*, 2020, **321**, 145–158.
2 N. A. Silva, N. Sousa, R. L. Reis and A. J. Salgado, *Prog. Neurobiol.*, 2014, **114**, 25–57.
3 J. Ruschel, F. Hellal, K. C. Flynn, S. Dupraz, D. A. Elliott, A. Tedeschi, M. Bates, C. Sliwinski, G. Brook, K. Dobrindt, M. Peitz, O. Brüstle, M. D. Norenberg, A. Blesch, N. Weidner, M. B. Bunge, J. L. Bixby and F. Bradke, *Science*, 2015, **348**, 347–352.
4 N. Nagoshi, H. Nakashima and M. Fehlings, *Molecules*, 2015, **20**, 7775–7789.
5 J. Wilcox, D. Cadotte and M. Fehlings, *Neurosci. Lett.*, 2012, **519**, 93–102.
6 T. Patel, J. Millignan and J. Lee, *J. Spinal Cord Med.*, 2017, **40**, 54–61.
7 A. Ulndreaj, A. Badner and M. G. Fehlings, *F1000Research*, 2017, **6**, 1907.
8 R. Shultz and Y. Zhong, *Neural Regener. Res.*, 2017, **12**, 702.
9 Y. Choi, H. Kim, K. Shin, E. Kim, M. Kim, H. Kim, C. Park, Y. Jeong, J. Yoo, J. Lee, K. Chang, S. Kim and Y. Suh, *Neuropsychopharmacology*, 2007, **32**, 2393–2404.
10 S. Zhu, I. G. Stavrovskaya, M. Drozda, B. Y. S. Kim, V. Ona, M. Li, S. Sarang, A. S. Liu, D. M. Hartley, D. C. Wu, S. Gullans, R. J. Ferrante, S. Przedborski, B. S. Kristal and R. M. Friedlander, *Nature*, 2002, **417**, 74–78.

11 K. Maier, D. Merkler, J. Gerber, N. Taheri, A. V. Kuhnert, S. K. Williams, C. Neusch, M. Bähr and R. Diem, *Neurobiol. Dis.*, 2007, **25**, 514–525.
12 B. W. Festoff, S. Ameenuddin, P. M. Arnold, A. Wong, K. S. Santacruz and B. A. Citron, *J. Neurochem.*, 2006, **97**, 1314–1326.
13 Y. D. Teng, H. Choi, R. C. Onario, S. Zhu, F. C. Desilets, S. Lan, E. J. Woodard, E. Y. Snyder, M. E. Eichler and R. M. Friedlander, *Proc. Natl. Acad. Sci. U. S. A.*, 2004, **101**, 3071–3076.
14 T. Yune, J. Lee, G. Jung, S. Kim, M. Jiang, Y. Kim, Y. Oh, G. Markelonis and T. Oh, *J. Neurosci.*, 2007, **27**, 7751–7761.
15 F. Abbaszadeh, S. Fakhri and H. Khan, *Pharmacol. Res.*, 2020, **160**, 105069.
16 S. Qian, Z. Wei, W. Yang, J. Huang, Y. Yang and J. Wang, *Front. Oncol.*, 2022, **12**, 985363.
17 J. He, J. Mao, L. Hou, S. Jin, X. Wang, Z. Ding, Z. Jin, H. Guo and R. Dai, *Exp. Anim.*, 2021, **70**, 21–0028.
18 H.-S. Kim and Y.-H. Suh, *Behav. Brain Res.*, 2009, **196**, 168–179.
19 A. M. Martins, J. M. Marto, J. L. Johnson and E. M. Graber, *Antibiotics*, 2021, **10**, 757.
20 F. Pinelli, F. Pizzetti, V. Veneruso, E. Petillo, M. Raghunath, G. Perale, P. Veglianese and F. Rossi, *Biomedicines*, 2022, **10**, 1673.
21 F. Rossi, G. Perale, S. Papa, G. Forloni and P. Veglianese, *Expert Opin. Drug Delivery*, 2013, **10**, 385–396.
22 Y. Hu, X. Chen, Z. Li, S. Zheng and Y. Cheng, *J. Biomed. Nanotechnol.*, 2020, **16**, 54–64.
23 I. Khan, A. Gothwal, A. K. Sharma, P. Kesharwani, L. Gupta, A. K. Iyer and U. Gupta, *Crit. Rev. Ther. Drug Carrier Syst.*, 2016, **33**, 159–193.
24 Y. Cui, X. Li, K. Zeljic, S. Shan, Z. Qiu and Z. Wang, *ACS Appl. Mater. Interfaces*, 2019, **11**, 38190–38204.
25 C. Huang, C. Fu, Z.-P. Qi, W.-L. Guo, D. You, R. Li and Z. Zhu, *Artif. Cells, Nanomed., Biotechnol.*, 2020, **48**, 1010–1021.
26 H. Xue, Y. Ju, X. Ye, M. Dai, C. Tang and L. Liu, *Int. J. Biol. Macromol.*, 2024, **254**, 128048.
27 Y. Luo, F. Xue, K. Liu, B. Li, C. Fu and J. Ding, *Mater. Des.*, 2021, **201**, 109484.
28 J. Wang, D. Li, C. Liang, C. Wang, X. Zhou, L. Ying, Y. Tao, H. Xu, J. Shu, X. Huang, Z. Gong, K. Xia, F. Li, Q. Chen, J. Tang and Y. Shen, *Small*, 2020, **16**(8), e1906415.
29 Y. Wang, M. Wu, L. Gu, X. Li, J. He, L. Zhou, A. Tong, J. Shi, H. Zhu, J. Xu and G. Guo, *Drug Delivery*, 2017, **24**, 391–401.
30 F. Lin, Y. Liu, W. Luo, S. Liu, Y. Wang, R. Gu, W. Liu and C. Xiao, *Int. J. Nanomed.*, 2022, **17**, 91–104.
31 J. Wang, D. Li, C. Liang, C. Wang, X. Zhou, L. Ying, Y. Tao, H. Xu, J. Shu, X. Huang, Z. Gong, K. Xia, F. Li, Q. Chen, J. Tang and Y. Shen, *Small*, 2020, **16**(8), e1906415.
32 L. Lei, Y. Bai, X. Qin, J. Liu, W. Huang and Q. Lv, *Gels*, 2022, **8**, 301.
33 M. Su, L. Ruan, X. Dong, S. Tian, W. Lang, M. Wu, Y. Chen, Q. Lv and L. Lei, *Int. J. Biol. Macromol.*, 2023, **227**, 472–492.
34 Z. Jia, H. Zeng, X. Ye, M. Dai, C. Tang and L. Liu, *Heliyon*, 2023, **9**, e19933.
35 D. Silva, R. A. Sousa and A. J. Salgado, *Mater. Today Bio*, 2021, **9**, 100093.
36 B. Jeong, S. W. Kim and Y. H. Bae, *Adv. Drug Delivery Rev.*, 2012, **64**, 154–162.
37 A. Navaei, D. Truong, J. Heffernan, J. Cutts, D. Brafman, R. W. Sirianni, B. Vernon and M. Nikkhah, *Acta Biomater.*, 2016, **32**, 10–23.
38 X. Qin, Y. Xu, X. Zhou, T. Gong, Z.-R. Zhang and Y. Fu, *Acta Pharm. Sin. B*, 2021, **11**, 835–847.
39 A. J. de Graaf, I. I. Azevedo Próspero dos Santos, E. H. E. Pieters, D. T. S. Rijkers, C. F. van Nostrum, T. Vermonden, R. J. Kok, W. E. Hennink and E. Mastrobattista, *J. Controlled Release*, 2012, **162**, 582–590.
40 Y. Sun, Y. Bai, S. Liu, S. Cui and P. Xu, *IET Nanobiotechnol.*, 2023, **2023**, 1–9.
41 M. Xu, Y. Mou, M. Hu, W. Dong, X. Su, R. Wu and P. Zhang, *Asian J. Pharm. Sci.*, 2018, **13**, 373–382.
42 T. Yi, G. Zhuang and Y. Wang, *Arq. Bras. Med. Vet. Zootec.*, 2022, **74**, 641–648.
43 X. Chen, J. Chen, B. Li, X. Yang, R. Zeng, Y. Liu, T. Li, R. J. Y. Ho and J. Shao, *J. Colloid Interface Sci.*, 2017, **490**, 542–552.
44 L. Li, Y. Li, C. Miao and R. Liu, *Adv. Polym. Technol.*, 2020, **2020**, 1–7.
45 X. Li, X. Xia, J. Zhang, M. Adu-Frimpong, X. Shen, W. Yin, Q. He, W. Rong, F. Shi, X. Cao, H. Ji, E. Toreniyazov, Q. Wang, J. Yu and X. Xu, *J. Pharm. Sci.*, 2023, **112**, 148–157.
46 D. Gao, S. Tang and Q. Tong, *Int. J. Nanomed.*, 2012, **7**, 3517–3526.
47 M. Adu-Frimpong, C. K. Firempong, E. Omari-Siaw, Q. Wang, Y. M. Mukhtar, W. Deng, Q. Yu, X. Xu and J. Yu, *Drug Dev. Res.*, 2019, **80**, 230–245.
48 H. Zhang, Q. Wang, C. Sun, Y. Zhu, Q. Yang, Q. Wei, J. Chen, W. Deng, M. Adu-Frimpong, J. Yu and X. Xu, *Pharmaceutics*, 2019, **11**, 107.
49 Y. Xue, Y. Liao, H. Wang, S. Li, Z. Gu, M. Adu-Frimpong, J. Yu, X. Xu, H. D. C. Smyth and Y. Zhu, *J. Sci. Food Agric.*, 2023, **103**, 3628–3637.
50 L. Lu, Y. Wang, M. Cao, M. Chen, B. Lin, X. Duan, F. Zhang, J. Mao, X. Shuai and J. Shen, *RSC Adv.*, 2017, **7**, 15041–15052.
51 Y. Mao, X. Li, G. Chen and S. Wang, *J. Pharm. Sci.*, 2016, **105**, 194–204.
52 M.-T. Sheu, H.-J. Jhan, C.-Y. Su, L.-C. Chen, C.-E. Chang, D.-Z. Liu and H.-O. Ho, *Colloids Surf., B*, 2016, **143**, 260–270.
53 C. Al Sabbagh, J. Seguin, E. Agapova, D. Kramerich, V. Boudy and N. Mignet, *Eur. J. Pharm. Biopharm.*, 2020, **157**, 154–164.
54 H. Li, X. Meng, Y. Zhang, M. Guo and L. Li, *Molecules*, 2023, **28**, 7319.
55 S. Kamiloglu, G. Sari, T. Ozdal and E. Capanoglu, *Food Front.*, 2020, **1**, 332–349.
56 S. Li, J. Zhou, J. Zhang, D. Wang and J. Ma, *Saudi J. Biol. Sci.*, 2019, **26**, 2122–2126.
57 Y. D. Teng, H. Choi, R. C. Onario, S. Zhu, F. C. Desilets, S. Lan, E. J. Woodard, E. Y. Snyder, M. E. Eichler and R. M. Friedlander, *Proc. Natl. Acad. Sci. U. S. A.*, 2004, **101**, 3071–3076.

58 V. Krishna, H. Andrews, X. Jin, J. Yu, A. Varma, X. Wen and M. Kindy, *J. Visualized Exp.*, 2013, **17**(78), 50111.
59 A. Singh, L. Krisa, K. L. Frederick, H. Sandrow-Feinberg, S. Balasubramanian, S. K. Stackhouse, M. Murray and J. S. Shumsky, *J. Neurosci. Methods*, 2014, **226**, 124–131.
60 J. Zhang, H. Ge, J. Li, L. Chen, J. Wang, B. Cheng and Z. Rao, *Regener. Ther.*, 2023, **24**, 180–189.
61 L. Luo, A. A. Albashari, X. Wang, L. Jin, Y. Zhang, L. Zheng, J. Xia, H. Xu, Y. Zhao, J. Xiao, Y. He and Q. Ye, *Stem Cells Int.*, 2018, **2018**, 1–13.
62 H. Song, H. Geng, J. Ruan, K. Wang, C. Bao, J. Wang, X. Peng, X. Zhang and D. Cui, *Nanoscale Res. Lett.*, 2011, **6**, 354.
63 Y.-C. Kuo and H.-W. Yu, *Colloids Surf., B*, 2011, **84**, 253–258.
64 T. N. S. Sulaiman, D. Larasati, A. K. Nugroho and S. Choiri, *Adv. Pharm. Bull.*, 2019, **9**, 382–392.
65 D.-L. Fang, Y. Chen, B. Xu, K. Ren, Z.-Y. He, L.-L. He, Y. Lei, C.-M. Fan and X.-R. Song, *Int. J. Mol. Sci.*, 2014, **15**, 3373–3388.
66 Y. Lu, E. Zhang, J. Yang and Z. Cao, *Nano Res.*, 2018, **11**, 4985–4998.
67 O. A. A. Ahmed and S. M. Badr-Eldin, *Int. J. Pharm.*, 2020, **588**, 119778.
68 G. Soliman and F. Winnik, *Macromol. Biosci.*, 2010, **10**, 278–288.
69 A. D. Holmkvist, A. Friberg, U. J. Nilsson and J. Schouenborg, *Int. J. Pharm.*, 2016, **499**, 351–357.
70 L. Treuel, X. Jiang and G. U. Nienhaus, *J. R. Soc., Interface*, 2013, **10**, 20120939.
71 Q. Wang, N. Wei, X. Liu, A. Chang and K. Qian Luo, *Oncotarget*, 2017, **8**, 12013–12030.
72 L. Lei, Y. Bai, X. Qin, J. Liu, W. Huang and Q. Lv, *Gels*, 2022, **8**, 301.
73 V. Perumal, A. R. Ravula, A. Agas, A. Gosain, A. Aravind, P. M. Sivakumar, S. S. I, K. Sambath, S. Vijayaraghavalu and N. Chandra, *Brain Sci.*, 2023, **13**, 402.
74 X.-Q. Zheng, J.-F. Huang, J.-L. Lin, Y.-X. Zhu, M.-Q. Wang, M.-L. Guo, X.-J. Zan and A.-M. Wu, *Colloids Surf., B*, 2021, **199**, 111532.
75 E. Dráberová, L. Del Valle, J. Gordon, V. Marková, B. Smejkalová, L. Bertrand, J. P. de Chadarévian, D. P. Agamanolis, A. Legido, K. Khalili, P. Dráber and C. D. Katsetos, *J. Neuropathol. Exp. Neurol.*, 2008, **67**(4), 341–354.
76 V. Martinsen and P. Kursula, *Amino Acids*, 2022, **54**(1), 99–109.
77 D. Chung, A. Shum and G. Caraveo, *Front. Cell Dev. Biol.*, 2020, **8**, 567537.
78 Y. Hoshino, T. Okuno, D. Saigusa, K. Kano, S. Yamamoto, H. Shindou, J. Aoki, K. Uchida, T. Yokomizo and N. Ito, *FASEB J.*, 2022, **36**(4), e22236.
79 A. Bernal and L. Arranz, *Cell. Mol. Life Sci.*, 2018, **75**(12), 2177–2195.